



Night-time NO emissions strongly suppress chlorine and nitrate radical formation during the winter in Delhi

Sophie L. Haslett^{1,2}, David M. Bell³, Varun Kumar^{3†}, Jay G. Slowik³, Dongyu S. Wang³, Suneeti Mishra⁴, Neeraj Rastogi⁵, Atinderpal Singh^{5‡}, Dilip Ganguly⁶, Joel Thornton⁷, Feixue Zheng⁸, Yuanyuan Li⁹, Wei Nie⁹, Yongchun Liu⁸, Wei Ma⁸, Chao Yan¹⁰, Markku Kulmala^{8,9,10}, Kaspar R. Daellenbach¹⁰, David Hadden^{1,2}, Urs Baltensperger³, Andre S. H. Prevot³, Sachchida N. Tripathi⁴ and Claudia Mohr^{1,2§}

¹Department of Environmental Science, Stockholm University; Stockholm, Sweden.

²Bolin Centre for Climate Research; Stockholm, Sweden.

³Laboratory of Atmospheric Chemistry, Paul Scherrer Institute; 5232 Villigen PSI, Switzerland.

10 ⁴Department of Civil Engineering, Indian Institute of Technology Kanpur; Kanpur, India.

⁵Geosciences Division, Physical Research Laboratory; Ahmedabad, India.

⁶Centre for Atmospheric Sciences, Indian Institute of Technology Delhi; New Delhi, India.

⁷Department of Atmospheric Sciences, University of Washington; Seattle, USA.

15 ⁸Aerosol and Haze Laboratory, Beijing Advanced Innovation Centre for Soft Matter Science and Engineering, Beijing University of Chemical Technology; Beijing, 100029, China.

⁹Joint International Research Laboratory of Atmospheric and Earth System Sciences, School of Atmospheric Sciences, Nanjing University; 210023 Nanjing, China.

¹⁰Institute for Atmospheric and Earth System Research/Physics, Faculty of Science, University of Helsinki; Helsinki, Finland.

20 *Correspondence to:* Claudia Mohr (claudia.mohr@psi.ch), Sachchida Tripathi (snt@iitk.ac.in), Sophie Haslett (sophie.haslett@aces.su.se)

[†]Now at: Institut National de l'Environnement Industriel et des Risques (INERIS), Parc Technologique ALATA, 60550 Vemeuil-en-Halatte, France.

[‡]Now at: Department of Environmental Studies, University of Delhi; Delhi 110007, India.

25 [§]Now at: Laboratory of Atmospheric Chemistry, Paul Scherrer Institute; 5232 Villigen PSI, Switzerland

Abstract. Atmospheric pollution in urban regions is highly influenced by oxidants due to their important role in the formation of secondary organic aerosol (SOA) and smog. These include the nitrate radical (NO₃), which is typically considered a night-time oxidant, and the chlorine radical (Cl), an extremely potent oxidant that can be released in the morning in chloride-rich environments as a result of nocturnal build-up of nitryl chloride (ClNO₂). Chloride makes up a higher percentage of particulate matter in Delhi than has been observed anywhere else in the world, which results in Cl having an unusually strong influence in this city. Here, we present observations and model results revealing that atmospheric chemistry in Delhi exhibits an unusual diel cycle, controlled by high concentrations of NO during the night. As a result of this, the formation of both NO₃ and dinitrogen pentoxide (N₂O₅), a precursor of ClNO₂ and thus Cl, are suppressed at night and increase to unusually high levels during the day. Our results indicate that a substantial reduction in night-time NO has the potential to increase both nocturnal oxidation via NO₃ and the production of Cl during the day.

30
35



1 Introduction

40 Delhi is one of the world's most polluted cities, and experiences its most severe pollution episodes during winter due to
stagnant meteorology and a compressed boundary layer (Guttikunda and Gurjar, 2012). Industry, agricultural burning, brick
kilns and traffic contribute substantially towards urban haze, in addition to widespread small-scale sources such as cooking
emissions, and waste and fuel burning (Rai et al., 2020; Guttikunda and Calori, 2013; Lalchandani et al., 2021; Pant et al.,
2015). Many of these are known to emit large quantities of chlorine (Rai et al., 2020; Gunthe et al., 2021; Zhang et al.,
45 2022).

Consequently, particulate chloride concentrations in Delhi are higher than anywhere else in the world where measurements
have been made. Chloride makes up around 10% of sub-micron particulate matter (Pant et al., 2015; Gunthe et al., 2021;
Gani et al., 2019; Tobler et al., 2020), and from our observations as much as 38% in some cases, compared with 4% during
50 the winter in Beijing (Zhang et al., 2020). The ramifications of this are only now beginning to be understood. For example,
new research has shown that chloride significantly impacts haze and fog formation in Delhi as a result of enhanced water
uptake (Gunthe et al., 2021). The severe consequences for human health are made all the more critical by the city's
extremely high population density (11,000 people km⁻² in 2011 (Joshi, 2011)).

55 High levels of particulate chloride can result in production of the chlorine radical (Cl), a highly reactive oxidant. Many
volatile organic compounds (VOCs) are oxidised by Cl at rates far exceeding that of the hydroxyl radical (OH) (Spicer et al.,
1998; Osthoff et al., 2008), the main atmospheric oxidant, meaning that even low Cl concentrations substantially increase
atmospheric reactivity. This can in turn increase secondary organic aerosol, SOA (Dhulipala et al., 2019; Wang and
Hildebrandt Ruiz, 2018) and therefore urban haze formation.

60 In the urban environment, Cl is extracted from particle-phase chloride when both nitrogen dioxide (NO₂) and ozone (O₃) are
present. Reactions between NO₂ and O₃ produce the nitrate radical (NO₃), another prominent atmospheric oxidant, which
forms an equilibrium with dinitrogen pentoxide (N₂O₅). Heterogeneous reactions between gaseous N₂O₅ and particulate
chloride produce nitryl chloride (ClNO₂). Due to both the instability of NO₃ in daylight and the fast reaction between NO₃ and
65 NO (Table S1), N₂O₅ and NO₃ are commonly depleted during the day and increase at night (Wang et al., 2017). This pattern
promotes the accumulation of night-time ClNO₂. After sunrise, ClNO₂ is photolysed and Cl liberated.

Here, we present evidence that this diel cycle is inverted in Delhi, with NO₃ and N₂O₅ being present primarily during the day.
Observations of N₂O₅ and ClNO₂ were carried out using an iodide chemical ionisation mass spectrometer fitted with a filter



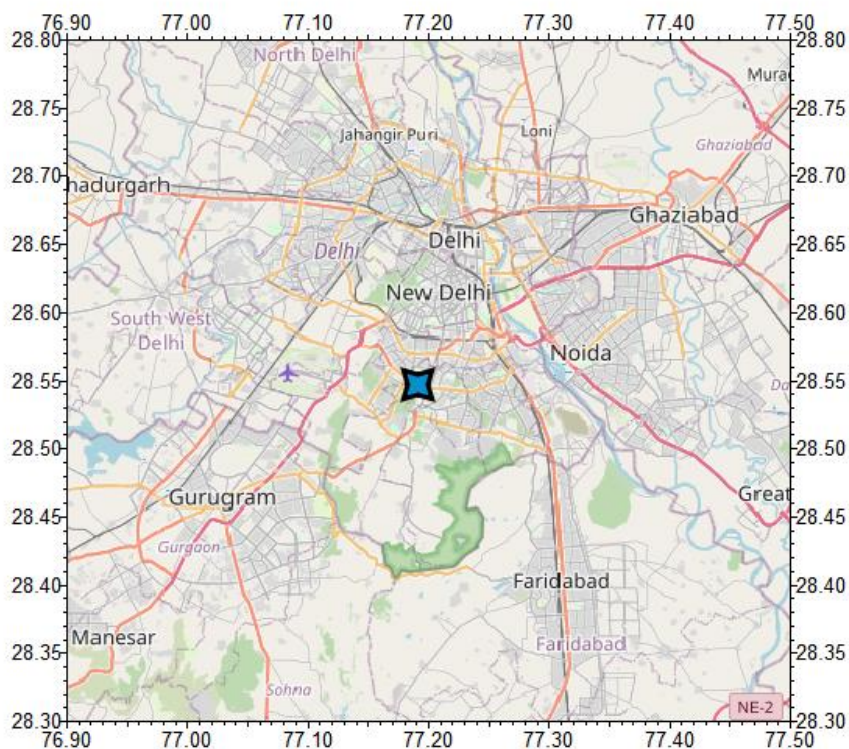
70 inlet for gases and aerosols (FIGAERO-CIMS) in January and February 2019, as part of a larger-scale effort to characterise
physical and chemical properties of Delhi's urban haze (Lalchandani et al., 2021; Rai et al., 2020; Singh et al., 2021a; Kumar
et al., 2022). During the campaign, we observed particulate chloride loadings in excess of $100 \mu\text{g m}^{-3}$ on several occasions.
Almost no N_2O_5 was observed at night, and daytime concentrations were in large excess compared with the few other places
75 2006)). Consequently, the concentrations of ClNO_2 formed were much lower than might have been expected considering the
high chloride loadings.

2 Methods

2.1 Field campaign and sampling site

The field study was carried out at the Department of Atmospheric Science at the Indian Institute of Technology in Delhi (IITD;
80 28.54°N , 77.19°E) during January and February 2019. Measurements were taken from 11 January – 5 February. Instruments
were installed in a temperature-controlled fourth-floor laboratory.

The site is surrounded by a mixture of residential, commercial and educational buildings. It is situated in the IITD campus,
which also contains a number of green spaces. Delhi's outer ring-road is located around 80 m to the north of the site, and a
85 larger arterial road can be found around 1 km ESE of the site. The site is a representative background urban site.
Measurements took place during the winter season, with temperatures ranging from around 10°C during the coolest night to
 30°C on the warmest day. Relative humidity ranged from 30% to 100%. More detail on the campaign site itself and the
aerosol and gas-phase instrumentation can be found in other publications from this campaign (Lalchandani et al., 2021; Rai
et al., 2020; Singh et al., 2021b; Wang et al., 2020; Kumar et al., 2022).



90

Figure 1: Map of the field site location at the Indian Institute of Technology in Delhi. (Map data © [OpenStreetMap](https://openstreetmap.org/) 2023. Distributed under the Open Data Commons Open Database License (OdbL) v1.0.)

2.2 The FIGAERO-CIMS

A high-resolution iodide-adduct chemical ionisation mass spectrometer with a filter inlet for particles and gases (FIGAERO-
95 CIMS) (Lopez-Hilfiker et al., 2014) (Aerodyne Research, Billerica) was used to measure N_2O_5 , $ClNO_2$ and oxygenated organic compounds. This method uses the negative iodide ion (I^-) as a reagent, which is produced by passing a dry nitrogen flow (1.5 lpm) over a methyl-iodide permeation tube, followed by an X-ray ioniser. This ionised ion flow interacts with incoming sample air in the ion molecular region (IMR), which is kept at 250 mbar, creating charged products that are identified as clusters containing I^- in the time-of-flight mass spectrometer. The FIGAERO inlet allows the gas phase to be sampled while
100 simultaneously collecting particles on a Teflon filter (PALL Zefluor, 2 μm pore size, 25 mm diameter). This filter was exposed to a sample air flow of 2 lpm for approximately 3 minutes, before being moved into the desorption position at the instrument inlet. In this position, it was heated gradually from room temperature to 200 °C, using a dry nitrogen flow at 2 lpm, before being held at 200 °C for 20 minutes and then cooled back down to room temperature over the course of 15 minutes. During the heating process, compounds that vaporise at temperatures below 200 °C desorb from the filter, with the quantity of each
105 compound growing as the temperature increases and then peaking at the temperature $T_{max,i}$, which differs for each compound



i. The temperature at which the maximum amount of a compound desorbs from the filter is related to the compound's volatility (Lopez-Hilfiker et al., 2014; Thornton et al., 2020). The total signal for each compound from each heating event was found by integrating the signal from the beginning of the heating period to the beginning of the cooling period.

110 Between particle-phase desorption periods, the gas phase was sampled directly by the FIGAERO-CIMS for approximately 20
minutes. For this study, these 20-minute periods have been averaged, providing averaged datapoints at a frequency of one
every 60-90 minutes while the instrument was running. Air samples were drawn at 3.5 lpm through the inlet, approximately 2
lpm of which entered the IMR, with the rest being included only to reduce residence time, and so pumped away. The N₂O₅
and ClNO₂ ions were observed clustered with I⁻ at 235 amu (*m/z* 235) and *m/z* 208, respectively (Slusher et al., 2004; Kercher
115 et al., 2009).

Background measurements were carried out 26 times for the particle phase and 6 times for the gas phase throughout the
campaign. For the particle phase, a clean, pre-heated Teflon filter (PALL Zefluor, 2 μm pore size, 25 mm diameter) was
inserted into the nitrogen flow and the standard heating procedure described above was carried out. The results from these
120 gave an indication of the instrument background, and the integrated signal for each compound was subtracted from the
integrated signal for each particle-phase measurement. In the gas phase, zero air gas was passed directly into the inlet and the
background was measured.

Particle-phase sampling for the FIGAERO-CIMS was conducted via a ½-inch outer diameter (0.35 inch inner diameter)
125 stainless steel tube of 1.5 m length (2 lpm, 2.8 s residence time) and gas-phase sampling was via a ¼-inch outer diameter (0.2
inch inner diameter) polyfluoroalkoxy- (PFA-) Teflon tube of around 2 m length (2 lpm, 1.2 s residence time).

Direct calibrations for N₂O₅ and ClNO₂ were not carried out in the field. The method used to quantify the FIGAERO-CIMS
signal for these compounds is detailed in the Supplementary Text S1 and Figs. S1 and S2.

130 **2.3 Other instrumentation**

An aerosol mass spectrometer (AMS; Aerodyne Research, Billerica) was used to quantify aerosol chloride, nitrate, ammonium,
sulfate and organic concentrations. The instrument setup for this campaign has been described in detail elsewhere (Kumar et
al., 2022). In brief, ambient air was sampled through an aerodynamic lens that limits sampling to particulate matter with a
diameter smaller than 1 μm (PM₁). Aerosol particles within the beam are flash vaporised at 600 °C, and the resulting vapours
135 ionised using electron impact ionisation. Ionised fragments pass into the time-of-flight mass spectrometer chamber and are
detected using a multi-channel plate (MCP) detector. This method can provide a quantitative measure of each species'
concentration in μg m⁻³. Ionisation efficiency calibrations were carried out before and after the campaign using 300-nm



ammonium nitrate particles. More information on this instrument's operation during this campaign has been reported by (Kumar et al., 2022).

140

NO_x measurements were carried out using a Serinus 40 Oxides of Nitrogen analyser (Ecotech). This instrument was calibrated at multiple concentration levels using the calibrator and standard gas cylinder before and after the campaign. The limit of detection was around 0.4 ppbv. A scanning mobility particle sizer (SMPS, GRIMM) provided size-binned measurements of the dry fine aerosol number concentration between 19 nm and 1 μm. A proton-transfer-reaction time-of-flight mass spectrometer (PTR, Ionicon Analytical G.m.b.H, Innsbruck, Austria) was used to measure VOCs.

145

Sampling for the NO_x analyser, O₃ analyser (Model 202, 2B Technologies) and SMPS was conducted via a 6 mm inner diameter stainless steel inlet of 3 m length, with an ambient particulate matter (APM_{2.5}) cyclone (BGI, Mesa Labs. Inc.) installed to remove larger particles (Kumar et al., 2022). The inlets extended around 1.5 m horizontally from the building's NNW side, around 12 m above the ground. Global radiation was measured on the roof of the building and other meteorological parameters including temperature, relative humidity, wind speed and wind direction were supplied by the Indian Meteorological Department (IMD).

150

2.4 0-dimensional chemical box model

A simple 0-dimensional (0-D) chemical box model was constructed in order to investigate the relative influence of N₂O₅ sources and sinks. The model was used to calculate concentrations of N₂O₅ and NO₃ based on values in the previous step, with a time step of 0.04 s and a “spin up” period of 24 hours. The reactions included in the model are outlined in Table S1 in the Supplement (Brown et al., 2003; Yan et al., 2019).

155

Here, $k_{\text{VOC},i}$ corresponds to the reaction rate constant of each individual volatile organic compound (VOC) in s⁻¹, and [VOC]_i to the concentration of the VOC, as measured by the PTR. The reaction rates for R6 and R7 rely on $c_{\text{N}_2\text{O}_5}$ and c_{NO_3} , the average molecular speed of an N₂O₅ or NO₃ molecule (\bar{c}_X), the uptake coefficients for N₂O₅ or NO₃, ($\gamma_{\text{N}_2\text{O}_5}$ and γ_{NO_3} , respectively) and the available aerosol surface area (S_A). These last two will be outlined in more detail below. The molecular speeds \bar{c}_X were calculated for each species X using Eq. 2 (Morgan et al., 2015), where k is Boltzmann's constant (1.38e-23 m² kg s⁻² K⁻¹), T represents the temperature in K and M_W is the molecular weight.

160

$$\bar{c}_X = \sqrt{\frac{8kT}{\pi M_W}} \quad (1)$$

165

Box model results were compared with results from a simple steady-state approach. Using the steady state approximation, it was possible to calculate NO₃ concentrations using Eq. 2 and N₂O₅ concentrations using Eq. 3 (Osthoff et al., 2006; Brown et al., 2005).



$$[\text{NO}_3]_{\text{calc}} = \frac{k_1[\text{NO}_2][\text{O}_3]}{k_3[\text{NO}] + j_4 + k_5 + k_6 K_{eq}[\text{NO}_2] + k_7} \quad (2)$$

170 $[\text{N}_2\text{O}_5]_{\text{calc}} = K_{eq}[\text{NO}_2][\text{NO}_3]_{\text{calc}} \quad (3)$

Here, square brackets denote the concentration of the respective compound in molecules cm^{-3} . Calculated concentrations of both species were found to agree closely with results from the box model, indicating that the steady-state approximation is reasonable in this case. Therefore, the simpler steady-state approach was used for the results presented here.

175 Time series data of NO, NO₃, O₃, VOCs, global radiation, temperature and wet particle surface area are used as direct inputs for reactions R1-R7 (see Supplement). The chemical compositions of VOCs included in the model were C₆H₆, C₇H₈, C₈H₁₀, C₉H₁₂, C₅H₈ and C₁₀H₁₆, which are all common urban VOCs that were observed in Delhi by the PTR. This model does not account for effects due to dilution, mixing or other atmospheric dynamics. However, much of this will already be accounted for due to changes in the input parameters (NO, NO₃, O₃ and VOCs). More details about the calculation of various input
180 parameters can be found in the Supplement.

The campaign averaged diel cycles were used for each input parameter. These diel averages for each compound were constructed by binning all measurements according to the time at which they were taken, and calculating the mean for each hour of the day across the whole campaign.

185 **2.5 The Framework for 0-D Atmospheric Modelling (F0AM)**

The F0AM model (Wolfe et al., 2016) is a 0-dimensional box model that can be used to simulate atmospheric chemistry systems. Here, we used the Master Chemical Mechanism (MCM) 3.3.1 chemistry, which was extended to include reactions for chlorine chemistry (Riedel et al., 2014). The latter included reactions of Cl with a series of VOCs, and further reactions of their oxidation products.

190

Observed values of NO_x, CO, HONO, HNO₃, ClNO₂, ClONO₂, HOCl, Cl₂ and a series of VOCs (Fig. S3, Table S2) were used as model inputs. A 24-hour diel cycle was modelled from 00:00, with a 48-hour “spin up” period. The model produced one datapoint per hour. We used the ‘MCM’ radiation model, which represents “typical” tropospheric conditions, but does not reflect variability in the ozone column, surface albedo, aerosol optical depth and clouds (Wolfe et al., 2016). The modelled
195 diel cycle of O₃ was used to scale the model’s photolysis parameter by comparing the calculated O₃ with observed values, which resulted in a photolysis scaling factor of 0.25.

The model was used to estimate the concentrations of the oxidants OH, NO₃, and O₃, and to explore the relative importance of different oxidation compounds for oxidation of different VOCs, with varying contributions from Cl.

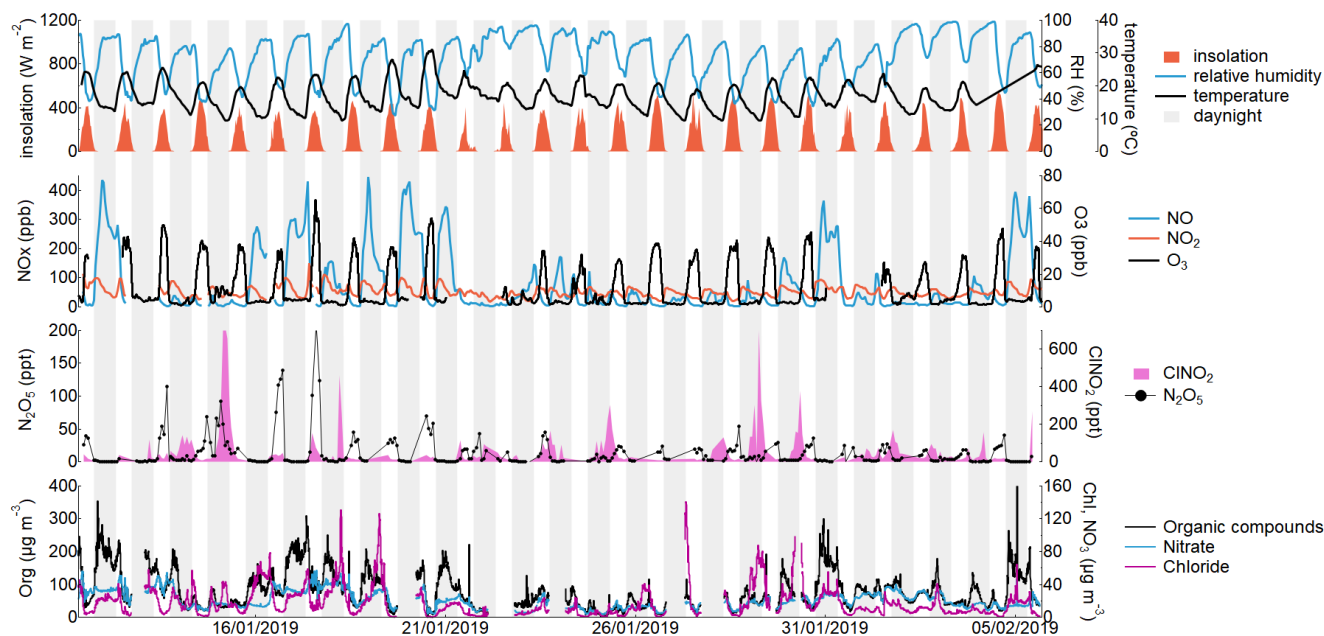


200 3. Results and discussion

3.1 Campaign overview

Figure 2 shows a time series of meteorological conditions and pollutant concentrations including NO_x , O_3 , ClNO_2 , N_2O_5 and particulate organics, nitrate and chloride during the field campaign in January and February 2019. During this period, the average daily maximum temperature was $22.7\text{ }^\circ\text{C}$, with a range from 19.0 to $31.1\text{ }^\circ\text{C}$, and the average night-time minimum temperature was $12.0\text{ }^\circ\text{C}$, ranging from 9.3 to $16.2\text{ }^\circ\text{C}$. Temperatures were reasonably stable throughout the campaign, with a slight peak around the 20th January. Relative humidities were higher at night, with an average low of 46.8% during the day and high of 89.1% at night.

Ozone concentrations reached an average 43 ppbv during the day, but were very low at night, usually just 2 or 3 ppbv. Concentrations of NO, in contrast, were highest during the night, with a mean of 84 ppbv in comparison with 22 ppbv during the day. This is an unusual feature and is likely a consequence of more heavy duty vehicles using the roads at night due to daytime restrictions (Tobler et al., 2020), in addition to low nocturnal O_3 levels limiting the conversion of NO to NO_2 . Less diurnal difference was shown by NO_2 , which averaged around 36 ppbv throughout the campaign, with small peaks in the morning and the evening. Particulate organic concentrations were very high during night-time periods, regularly exceeding $200\text{ }\mu\text{g m}^{-3}$, and reducing to an average of $61\text{ }\mu\text{g m}^{-2}$ during the day, primarily as a result of dilution caused by the change in boundary layer height. Particulate chloride was enhanced in the early mornings, sometimes exceeding concentrations of $100\text{ }\mu\text{g m}^{-3}$. These values are consistent with previous studies carried out in Delhi, which have shown the city to have among the highest levels of particulate chloride measured anywhere in the world (Gani et al., 2019; Gunthe et al., 2021).



220

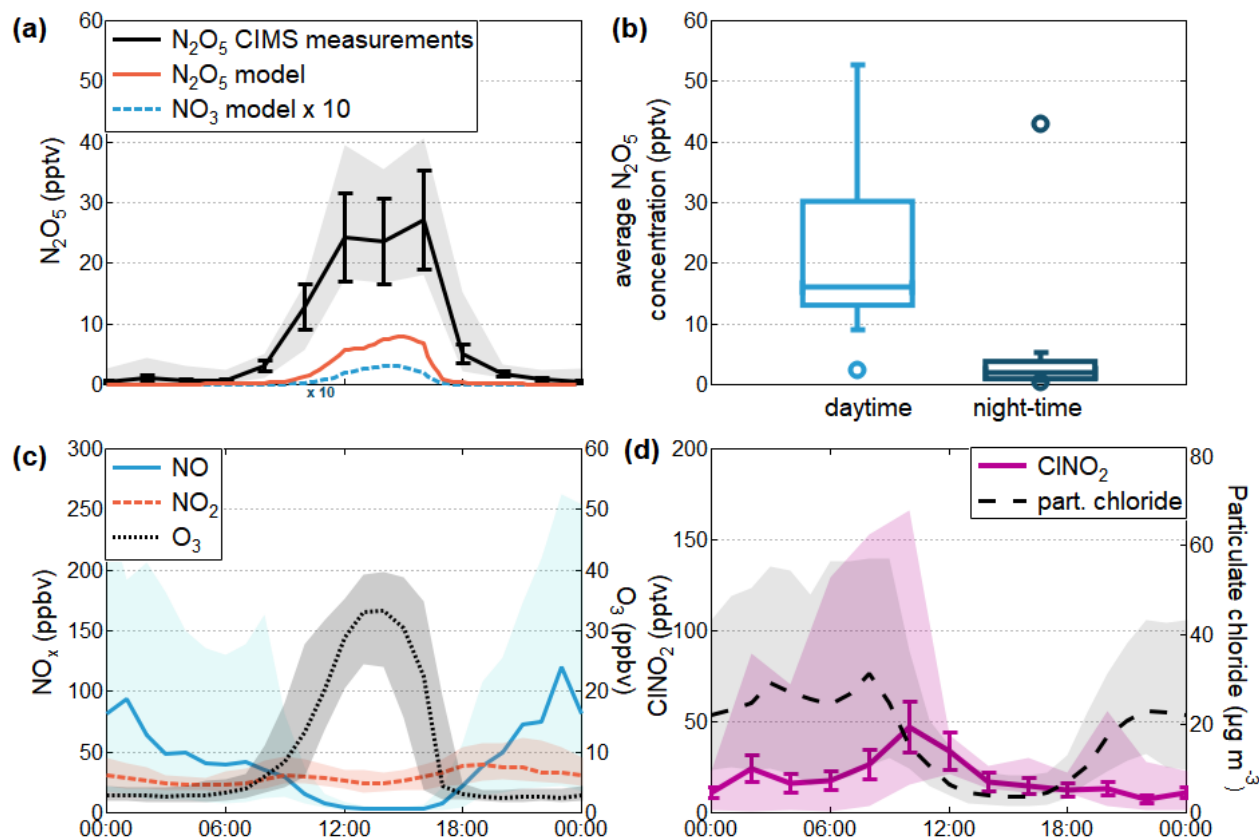
Figure 2: Full campaign time series of key species and meteorological parameters. Grey and white backgrounds represent night-time and daytime, respectively.

3.2 Unusual diel patterns in Delhi

Figure 3a shows the average diel cycle of N_2O_5 , as measured by the FIGAERO-CIMS from 11 January to 5 February 2019. The mean daytime concentration of N_2O_5 during the measurement period was 21.9 pptv (standard deviation 29.3 pptv; median 16.0 pptv), compared with a night-time mean of 4.4 (standard deviation 11.3 pptv; median 2.0 pptv; Fig. 3b). A simple 0-dimensional chemical box model was designed to investigate the driving factors behind this inverted N_2O_5 pattern in more detail. This simple model successfully recreated the shape of the N_2O_5 diurnal pattern observed in the FIGAERO-CIMS dataset (Fig. 3a), and indicated that NO_3 is likely to follow a similar diel cycle.

230

Model results demonstrate that the diurnal NO_3 and N_2O_5 patterns were influenced most strongly by NO. Our observations show high night-time concentrations of NO, which diminish considerably during the day (Fig. 3c). This pattern has been observed previously in Delhi and is generally attributed to the low, stable nocturnal boundary layer (Stewart et al., 2021) in combination with substantial NO_x sources, such as heavy-duty traffic and biomass burning, being strongly present at night (Mishra et al., 2023). These night-time NO emissions deplete O_3 to extremely low concentrations, leaving an excess of NO. Together, these effects ensure that the destruction of NO_3 by NO is at its highest during the night, while its production, which requires O_3 , is at its lowest. In contrast, the presence of O_3 and NO_2 during the day, coupled with little daytime NO, results in higher daytime concentrations of NO_3 and N_2O_5 being sustained than would typically be possible.



240

Figure 3: Median diel patterns for the key compounds explored in this study. (a) The median diel cycle of N_2O_5 measured by the FIGAERO-CIMS with the interquartile range shaded, alongside the N_2O_5 and NO_3 simulations from the 0D box model. Error bars indicate a potential 30% error in the estimated calibration constant. (b) Box plots showing the average N_2O_5 concentrations throughout the campaign during the day and the night as measured by the FIGAERO-CIMS, indicating that there is a distinct and consistent decrease in N_2O_5 concentrations at night. (c) The observed median diel patterns of the precursor species NO , NO_2 and O_3 with interquartile ranges shaded. (d) The observed diel pattern of $ClNO_2$ and particulate chloride throughout the campaign. The error bars here, as in (a), represent a 30% potential calibration error.

245

Our modelled N_2O_5 concentrations are around a two-thirds lower than those observed. Combined with the observed mid-morning peak in $ClNO_2$ (Fig 1d), this is an indication that night-time production of both N_2O_5 and $ClNO_2$ continues to some extent in the residual layer, decoupled from the urban canopy layer in which our measurements take place. After sunrise and the ensuing atmospheric instability, the N_2O_5 and $ClNO_2$ from the nocturnal residual layer is likely incorporated into the daytime mixed layer and transported by turbulence downwards to the measurement system (Fig. S4). Furthermore, it can be seen in Fig. S4 that night-time concentrations of $ClNO_2$ are highest with greater atmospheric mixing, supporting the hypothesis that during periods of poor atmospheric mixing the measurement system (which is relatively close to the ground level) is decoupled from air masses above the urban canopy layer that contain higher concentrations of $ClNO_2$. Based on the discrepancy between model and observations for N_2O_5 (Fig. 3a) and on the difference between average nocturnal concentrations and the

250

255



morning peak for ClNO_2 (Fig. 3d), we estimate that an average of approximately 18 ± 3 pptv of N_2O_5 and 12 ± 3 pptv of ClNO_2 are mixed from the residual layer into the surface layer from above in the mornings, increasing the overall influence of both species during the day.

260

In addition to model results, oxidation products observed by the FIGAERO-CIMS provide evidence both that Cl is an important oxidant in Delhi, and that oxidation with NO_3 takes place during the day. Chloroacetic acid ($\text{C}_2\text{H}_3\text{O}_2\text{Cl}$) has previously been designated a tracer compound to indicate the presence of Cl oxidation (Le Breton et al., 2018; Priestley et al., 2018) and was observed here, exhibiting a strong diurnal pattern (Fig. 4b). Similarly, a number of individual compounds that have previously been observed in conjunction with night-time NO_3 oxidation of monoterpenes were observed primarily as daytime species during this campaign, with the examples of $\text{C}_8\text{H}_{11}\text{NO}_7$ (Ye et al., 2021; Lee et al., 2016) and $\text{C}_{10}\text{H}_{15}\text{NO}_6$ (Ye et al., 2021; Boyd et al., 2015) displayed here (Fig. 4b). The nitrogen-containing organic compounds (CHON) that increased most strongly during the night were all found to be associated with primary biomass burning emissions (Mishra et al., 2023), not oxidation products (Fig. S5). The overall contribution of CHON as a fraction of total organics increased slightly during daylight hours (Fig. 4b), particularly in the gas phase, while results from other parts of the world have typically found the contribution of CHON to increase slightly at night as a result of NO_3 oxidation (Ye et al., 2021; Huang et al., 2019). Daytime peaks in NO_3 oxidation products will likely result from both daytime oxidation by NO_3 within the surface layer and the mixing down of products from nocturnal oxidation taking place within the elevated residual layer. Given that the other important urban oxidants, OH and O_3 , in addition to Cl, also display daytime maxima, all four key oxidants can be considered daytime species in this environment. As a corollary, there are no significant nocturnal oxidants in the surface layer.

275

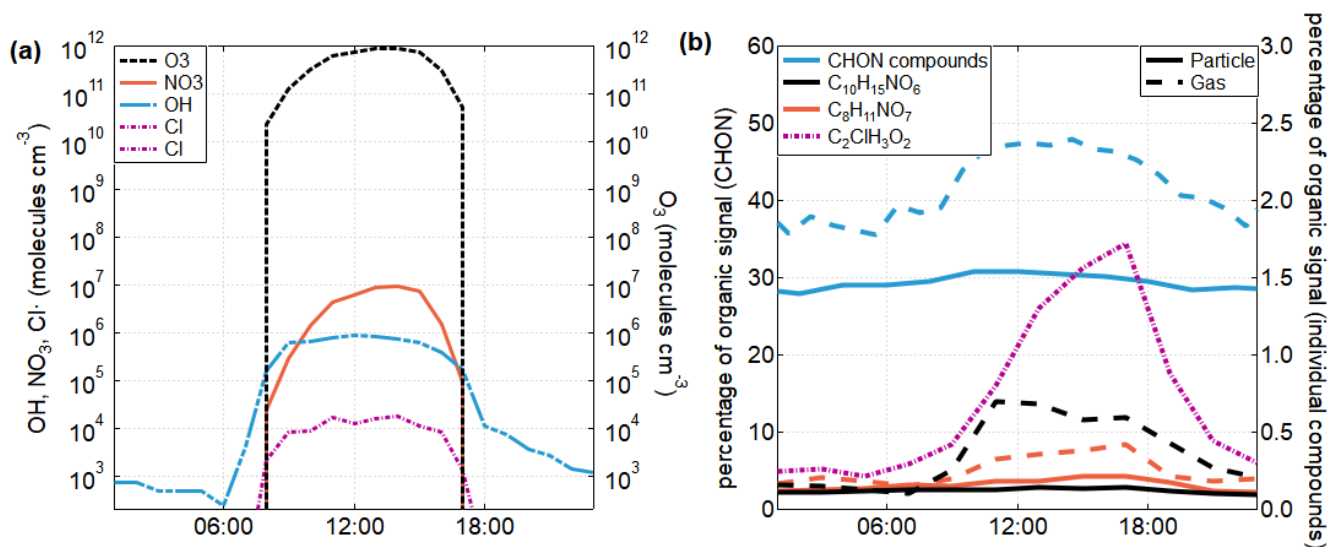


Figure 4: The diel cycles of key oxidants and oxidation products in Delhi. (a) The diel cycle of four key oxidants, O_3 , Cl, NO_3 and OH. The Cl concentration has been estimated from chlorine-containing species observed by the FIGAERO-CIMS (Methods).



280 **Estimated concentrations of the other three oxidants are calculated using the Framework for 0-D Atmospheric Modelling (F0AM)**
chemical box model (Wolfe et al., 2016) (Methods). (b) The diel cycles of total N-containing organics in the gas and particle phases
(blue) with selected compounds $C_8H_{11}NO_7$ (orange) and $C_{10}H_{15}NO_6$ (black) also displayed in both the gas and particle phases. These
two compounds, both associated with NO_3 oxidation, are most prevalent during the day when the NO_3 concentration peaks, while
compounds associated with biomass burning are more prevalent at night (Fig. S5). The diel cycle of $C_2H_3O_2Cl$, a known tracer of Cl
285 **chemistry, is shown in pink. These compounds were not calibrated, so here the percentage contribution of each compound or group**
of compounds towards the total organic signal is displayed on the y-axes.

One of the consequences of this shift away from night-time NO_3 within the urban canopy layer is that very little oxidation
from any oxidant takes place at the time when sub-micron particulate matter (PM_{10}) is at its most concentrated; our observations
show that PM_{10} more than doubles from day to night (Fig. S6a). As a result, the overall oxidation state of aerosol in Delhi is
very low. A previous investigation of the organic aerosol chemical speciation during this campaign using positive matrix
290 factorisation on aerosol mass spectrometer (AMS) and extractive electrospray ionisation mass spectrometer (EESI) data shows
that factors associated with oxidation reactions are enhanced during the day in Delhi, while particulate matter present during
the night is the least oxidised (Kumar et al., 2022). The average oxidation state of particulate matter during this campaign has
been found to be unusually low compared with a global dataset of FIGAERO-CIMS observations in different environments
(Huang et al., 2023). If the distribution of oxidants were to change, this would likely increase SOA mass in the region. Such a
295 change could come about if nocturnal NO were to decrease, thereby increasing nocturnal concentrations of NO_3 and N_2O_5 and
allowing larger quantities of $ClNO_2$, and therefore Cl radicals, to be produced.

3.3 The potential influence of changes to the diel pattern

Figure 5a shows the relationship between night-time average NO and N_2O_5 concentrations in Delhi. It can be seen here that,
as NO concentrations during the night decrease, the N_2O_5 produced increases substantially. Data from this campaign are
300 displayed alongside observations from Beijing, which were carried out during January 2020. Similar to Delhi, Beijing is a
polluted urban centre with a notable contribution from chloride in the particle phase, albeit around 17 times lower than Delhi,
on average, based on observations presented here. However, the concentrations of N_2O_5 in Beijing display a more typical diel
pattern, with higher values at night. Night-time N_2O_5 regularly exceeds 100 pptv in Beijing, while Delhi's generally remains
below 10 pptv. This comparison allows us to understand more about the impact of Delhi's unusual NO_x cycle on atmospheric
305 chemistry. Where the two cities have some overlap in night-time NO concentrations, the quantity of N_2O_5 produced at night
is roughly comparable. However, the majority of nights in Beijing have much lower NO concentrations than any observed in
Delhi; at these lower concentrations, much more N_2O_5 can be produced, in some cases reaching close to 1 ppbv. There is a
larger spread in N_2O_5 concentrations during nights with low NO, because other factors such as the amount of available NO_2
and O_3 also have an impact on N_2O_5 formation.

310

The World Health Organisation (WHO) published new air quality guidelines in 2021 (World Health Organization, 2021),
which include guideline 24-hour and annual thresholds of 25 and 10 $\mu g m^{-3}$ (~13.4 and 5.3 ppbv), respectively for NO_2 . Our
observations show that during the night in Delhi, NO makes up on average 64% of NO_x ($NO + NO_2$) (Fig. S6b). Approximate



night-time NO equivalent thresholds of around 23.8 ppbv in 24 hours or 9.4 ppbv annually can therefore be established. This
315 NO equivalent threshold is displayed in Fig. 5a and can be used to separate the data into two regimes, with nights above the
threshold being considered ‘high NO’ and those below ‘low NO’. The majority of nights in Delhi fall within the ‘high NO’
regime, while the majority of those in Beijing fall into the ‘low NO’ regime. Within the ‘high NO’ regime, the average N₂O₅
concentration across both datasets is 4.1 pptv, while in the ‘low NO’ regime, the average N₂O₅ concentration per night is 220
pptv. The overlap between NO concentrations in the two cities suggests that it is possible for changes in environmental
320 conditions to shift the atmosphere from one regime to the other: there were some nights during which high NO concentrations
in Beijing suppressed the formation of N₂O₅, and in Delhi during which low NO concentrations allowed more production of
N₂O₅. These results suggest that, if night-time NO emissions were to be reduced in line with WHO guidance, there would
likely be a substantial increase in the night-time production of N₂O₅.

325 The relationship between night-time N₂O₅ and ClNO₂ observations for both Delhi and Beijing can be seen in Fig. 5b. Larger
night-time concentrations of N₂O₅ result in the production of more ClNO₂, as it increases the number of interactions at the
surface of chloride-containing particles. These two datasets together show that, as the ambient concentration of particle-phase
chloride increases, this reaction is able to take place more readily and the ratio of ClNO₂ to N₂O₅ also increases. This results
in much higher quantities of ClNO₂ being produced in Delhi, with its higher particulate chloride, for a given concentration of
330 N₂O₅ than in Beijing. A linear regression line was fitted to the log of the Delhi dataset to demonstrate this relationship, which
has an r^2 of 0.58. This pattern indicates that, if night-time N₂O₅ concentrations in Delhi were to increase to values as high as
those found in Beijing, the high availability of particle-phase chloride could result in ClNO₂ production exponentially higher
than it is at present. Following the current trendline, an increase in night-time N₂O₅ to 115 pptv – the log-weighted average
from the Beijing dataset – would increase the ClNO₂ concentrations in Delhi to an average of 1450 pptv, two orders of
335 magnitude higher than the current log-weighted average of 14 pptv.

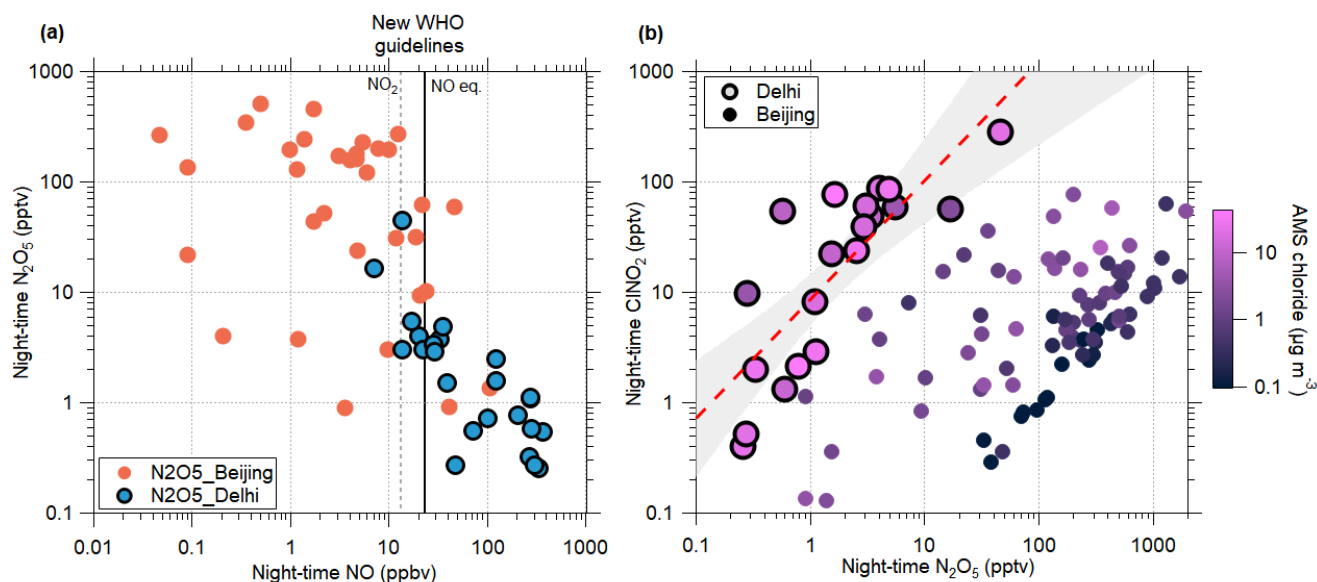


Figure 5: Relationships between night-time $ClNO_2$, N_2O_5 and NO. (A) Average nocturnal concentrations of N_2O_5 plotted against average nocturnal concentrations of NO, for our campaign results from Delhi and from measurements in Beijing from 2020. The new 24-hour WHO guideline for NO_2 concentrations is displayed by the dashed grey line, with the calculated NO equivalent shown by the solid black line. (B) Relationship between nocturnal $ClNO_2$ and N_2O_5 . Colouring shows the average particulate chloride concentration, as measured by the AMS. The red dashed line shows the least-squares regression line for the Delhi dataset, with 95% confidence intervals shown in grey. The equation for the line is given by the equation $\ln(ClNO_2 (pptv)) = 1.08 \ln(N_2O_5 (pptv)) + 2.16$. Datapoints from between 20:00 and 05:00 the following morning are included.

340

345

350

355

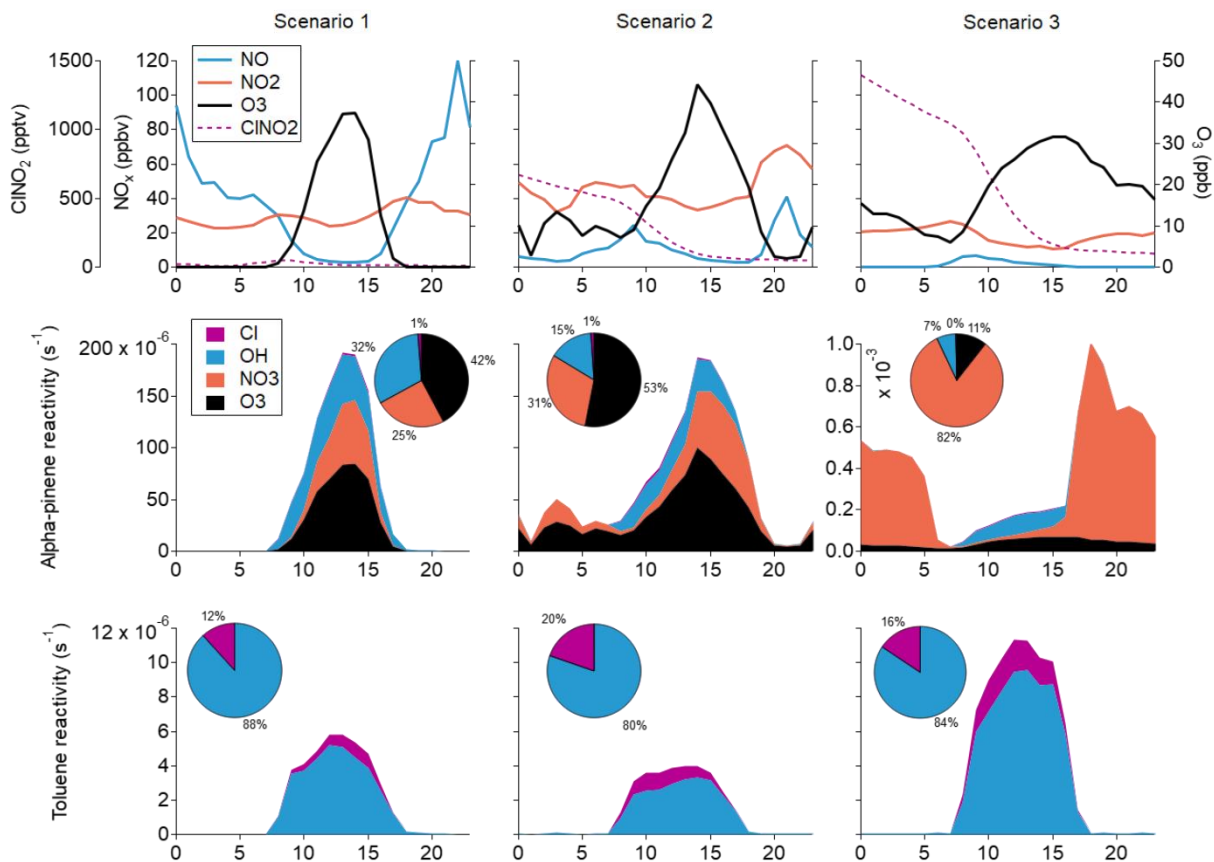
We used the FOAM box model (Wolfe et al., 2016; Riedel et al., 2014) to investigate the relative contributions of Cl and NO_3 radicals as oxidants for two common VOCs, alpha-pinene and toluene, under three simulated scenarios. In scenario 1, we used the average diel NO_x concentrations displayed in Fig. 3a as input parameters for the FOAM model. This represents the baseline case. Scenario 2 uses NO_x and O_3 data from a case study day on 15th January 2019. This date was chosen as it includes the night during the campaign that exhibited the lowest night-time NO and highest O_3 , leading to the production of a comparatively large amount of $ClNO_2$, which peaked at 715 pptv. Data were extracted between 18:00 on 14th January and 18:00 on 15th January 2019, replicated and concatenated to form a full diel cycle. This case study represents the most extreme example of the ‘low NO’ regime observed during our measurement period. Finally, scenario 3 features NO_x and O_3 input parameters that have been taken from the Beijing dataset displayed in Fig. 5 as a stand-in for a more conventional diel cycle in a similarly polluted city. Average sunrise and sunset times differed by only 11 and 13 minutes, respectively, between the two campaigns, which indicates that the timing of concentration changes is likely to be appropriate for the model. The NO and NO_2 maxima and diel patterns are comparable to those observed in Punjab, north of Delhi (Meidan et al., 2022), indicating that they are conceivable for the region. The Beijing dataset was used here because the maximum O_3 concentrations and sunrise and set times are more closely comparable with those in Delhi at this time of year. The concentration of $ClNO_2$ was fixed at the



beginning of the model run to the highest night-time value in scenario 2, and to 1.45 ppbv in scenario 3, which has been
360 calculated from the fit line in Fig. 5 based on measured N_2O_5 concentrations in Beijing. The ClNO_2 was then depleted
throughout the model run by photolysis, to create oxidising Cl radicals. Scenario 3 is not intended to be a prediction of future
atmospheric chemistry in Delhi. Rather, it represents a highly idealised scenario that can be used to explore the potential
ramifications of substantial changes to the NO_x and O_3 cycle in the context of Delhi's polluted and chlorine-rich environment.

365 The results of these model runs are shown in Fig. 6. In scenario 1, which represents the current situation in Delhi, Cl is
responsible for 12% of the toluene oxidation, indicating that it is already a major oxidant in the city. No NO_3 is produced
during the night in this scenario, but as a result of its presence during the day, 25% of the alpha-pinene oxidation is initiated
by NO_3 . During scenario 2, the higher ClNO_2 concentration results in almost a doubling of the proportion of toluene oxidised
by Cl to 20%. In addition, the slight increase in night-time NO_3 and O_3 results in some night-time oxidation of alpha-pinene
370 taking place. This indicates that night-time oxidation is taking place in Delhi, although it is largely restricted to nights that fall
within the 'low NO' regime. In this case, NO_3 is responsible for 31% of the alpha-pinene oxidation.

Scenario 3 shows a substantial increase in night-time oxidation from NO_3 and daytime oxidation from Cl, due to the large
nocturnal concentration of O_3 that is sustained, alongside the lack of NO. Here, the large increase in night-time NO_3 production,
375 coupled with the increase in VOC concentrations during the night, leads to NO_3 becoming the key oxidant for alpha-pinene,
accounting for 82% of its reactivity. Concerning the toluene reactivity, only 16% is initiated by Cl in this case, which is largely
due to the associated increase in OH oxidation. In fact, the Cl-initiated toluene reactivity in scenario 3 is almost double that of
scenario 2.



380 **Figure 6: The reactivity of toluene and alpha-pinene under three simulated scenarios. (A), (B) and (C) show the NO, NO₂, O₃ and CINO₂ concentrations for scenarios 1, 2 and 3, respectively. In all three cases, NO and NO₂ values in the model are held to the measurements, as is O₃ in scenarios 2 and 3. For CINO₂, the initial value is fixed and evolves throughout the model run for scenarios 2 and 3. (D), (E) and (F) indicate the reactivity of alpha-pinene in scenarios 1, 2 and 3 respectively, and (G), (H) and (I) the reactivity of toluene.**

385 4. Conclusions

The analysis presented here demonstrates that the diel cycles of the typically nocturnal species NO₃ and N₂O₅ are inverted during the winter in Delhi's surface layer. This is due to the presence of large concentrations of NO during the night, which depletes NO₃ and therefore results in both NO₃ and N₂O₅ consistently peaking during the day. This unique diel chemical pattern limits the formation of night-time CINO₂. Despite this constraint on CINO₂ formation, the extremely high particulate chloride loadings available in Delhi still result in enough Cl production for it to be an important atmospheric oxidant. Model simulations carried out here using the FOAM model demonstrate that the role of Cl as an oxidant of toluene could be more than 10 times higher if the diel cycle of NO_x were more representative of that observed in comparable urban atmospheres such as Beijing. Similarly, the role of NO₃ as an oxidant of alpha-pinene was shown to be around 30 times lower in Delhi than it would be if



the NO_x pattern were more typical. This is a particularly significant difference from the majority of urban centres, as NO_3
395 would otherwise be the only oxidant that is most prominent during the night, when the concentration of particulate matter is
at its highest.

A number of clean air policies, including the latest update to the WHO guidelines on ambient air pollution (World Health
Organization, 2021), emphasise the control of NO_x pollution in urban environments. This study highlights the complexity of
400 atmospheric chemistry in a highly-polluted urban environment. Given the delicate chemical balance in Delhi's winter
atmosphere, there is potential for significant changes in night-time NO pollution to result in increased production of NO_3 and
 N_2O_5 in the surface layer. Such a change could be initiated by, for example, a reduction in nocturnal vehicle emissions. Our
results indicate that both NO_3^- - and Cl -initiated oxidation could be substantially increased if the diurnal cycle for NO_x in Delhi
were more representative of that seen in other major cities; this would increase the formation of SOA and therefore worsen
405 urban haze. We strongly recommend careful monitoring of NO_x , O_3 and particulate chloride levels in Delhi, as there is potential
for disruption to the NO_x cycle. It is important for more research to be undertaken into this problem in order to understand the
potential ramifications in more depth.

Data availability. Data from this paper will be made available on the Bolin Centre Database.

410 **Author contributions.** The concept for this manuscript was established by SLH and CM, with input from DMB, JT, UB,
ASHP and SNT. Investigation and measurements were carried out by SLH, VK, DSW, SM, NR, AS, DG, FZ, YL, WN, YL,
WM, CY, KRD and CM. MK, UB, ASHP, SNT and CM acquired funding for this project. The writing was carried out by
SLH. Reviewing and editing was undertaken with input from all co-authors.

Acknowledgements. The research conducted in this paper was supported by the Knut and Alice Wallenberg Foundation
415 (project CLOUDFORM, grant no. 2017.0165). One of the corresponding authors (SNT) gratefully acknowledges the financial
support provided by the Central Pollution Control Board (CPCB), Government of India, to conduct this research under grant
no. AQM/Source apportionment_EPC Project/2017. We also acknowledge funding from the SDC Clean Air Project in India
(grant no. 7F-10093.01.04), the Swiss National Science Foundation (2000021_169787). KRD acknowledges support by the
Schweizerischer Nationalfonds (SNF) mobility grant (grant no. P2EZP2_181599) and Ambizione grant (grant no.
420 PZPGP2_201992).

Competing interests. The authors declare that they have no conflict of interest.



References

- 425 Boyd, C. M., Sanchez, J., Xu, L., Eugene, A. J., Nah, T., Tuet, W. Y., Guzman, M. I., and Ng, N. L.: Secondary organic aerosol formation from the β -pinene+NO₃ system: effect of humidity and peroxy radical fate, *Atmospheric Chemistry and Physics*, 15, 7497–7522, <https://doi.org/10.5194/acp-15-7497-2015>, 2015.
- Brown, S. S., Stark, H., and Ravishankara, A. R.: Applicability of the steady state approximation to the interpretation of atmospheric observations of NO₃ and N₂O₅, *Journal of Geophysical Research: Atmospheres*, 108, <https://doi.org/10.1029/2003JD003407>, 2003.
- 430 Brown, S. S., Osthoff, H. D., Stark, H., Dubé, W. P., Ryerson, T. B., Warneke, C., de Gouw, J. A., Wollny, A. G., Parrish, D. D., Fehsenfeld, F. C., and Ravishankara, A. R.: Aircraft observations of daytime NO₃ and N₂O₅ and their implications for tropospheric chemistry, *Journal of Photochemistry and Photobiology A: Chemistry*, 176, 270–278, <https://doi.org/10.1016/j.jphotochem.2005.10.004>, 2005.
- 435 Dhulipala, S. V., Bhandari, S., and Hildebrandt Ruiz, L.: Formation of oxidized organic compounds from Cl-initiated oxidation of toluene, *Atmospheric Environment*, 199, 265–273, <https://doi.org/10.1016/j.atmosenv.2018.11.002>, 2019.
- Gani, S., Bhandari, S., Seraj, S., Wang, D. S., Patel, K., Soni, P., Arub, Z., Habib, G., Hildebrandt Ruiz, L., and Apte, J. S.: Submicron aerosol composition in the world's most polluted megacity: the Delhi Aerosol Supersite study, *Atmospheric Chemistry and Physics*, 19, 6843–6859, <https://doi.org/10.5194/acp-19-6843-2019>, 2019.
- 440 Geyer, A., Alicke, B., Ackermann, R., Martinez, M., Harder, H., Brune, W., Carlo, P. di, Williams, E., Jobson, T., Hall, S., Shetter, R., and Stutz, J.: Direct observations of daytime NO₃: Implications for urban boundary layer chemistry, *Journal of Geophysical Research: Atmospheres*, 108, <https://doi.org/10.1029/2002JD002967>, 2003.
- 445 Gunthe, S. S., Liu, P., Panda, U., Raj, S. S., Sharma, A., Darbyshire, E., Reyes-Villegas, E., Allan, J., Chen, Y., Wang, X., Song, S., Pöhlker, M. L., Shi, L., Wang, Y., Kommula, S. M., Liu, T., Ravikrishna, R., McFiggans, G., Mickley, L. J., Martin, S. T., Pöschl, U., Andreae, M. O., and Coe, H.: Enhanced aerosol particle growth sustained by high continental chlorine emission in India, *Nature Geoscience*, 1–8, <https://doi.org/10.1038/s41561-020-00677-x>, 2021.
- Guttikunda, S. K. and Calori, G.: A GIS based emissions inventory at 1 km × 1 km spatial resolution for air pollution analysis in Delhi, India, *Atmospheric Environment*, 67, 101–111, <https://doi.org/10.1016/j.atmosenv.2012.10.040>, 2013.
- 450 Guttikunda, S. K. and Gurjar, B. R.: Role of meteorology in seasonality of air pollution in megacity Delhi, India, *Environ Monit Assess*, 184, 3199–3211, <https://doi.org/10.1007/s10661-011-2182-8>, 2012.
- Huang, W., Saathoff, H., Shen, X., Ramisetty, R., Leisner, T., and Mohr, C.: Chemical Characterization of Highly Functionalized Organonitrates Contributing to Night-Time Organic Aerosol Mass Loadings and Particle Growth, *Environ. Sci. Technol.*, 53, 1165–1174, <https://doi.org/10.1021/acs.est.8b05826>, 2019.
- 455 Huang, W., Wu, C., Gao, L., Gramlich, Y., Haslett, S. L., Thornton, J., Lopez-Hilfiker, F. D., Lee, B. H., Song, J., Saathoff, H., Shen, X., Ramisetty, R., Jiang, F., Vallon, M., and Mohr, C.: Variation in chemical composition and volatility of oxygenated organic aerosol in different rural, urban, and remote environments, In Prep, 2023.
- Joshi, V.: Census of India: Provisional population totals for census 2011, Directorate of Census Operations, Delhi, 2011.



- 460 Kercher, J. P., Riedel, T. P., and Thornton, J. A.: Chlorine activation by N₂O₅: simultaneous, in situ detection of ClNO₂ and N₂O₅ by chemical ionization mass spectrometry, *Atmospheric Measurement Techniques*, 2, 193–204, <https://doi.org/10.5194/amt-2-193-2009>, 2009.
- 465 Kumar, V., Giannoukos, S., Haslett, S. L., Tong, Y., Singh, A., Bertrand, A., Lee, C. P., Wang, D. S., Bhattu, D., Stefenelli, G., Dave, J. S., Puthussery, J. V., Qi, L., Vats, P., Rai, P., Casotto, R., Satish, R., Mishra, S., Pospisilova, V., Mohr, C., Bell, D. M., Ganguly, D., Verma, V., Rastogi, N., Baltensperger, U., Tripathi, S. N., Prévôt, A. S. H., and Slowik, J. G.: Highly time-resolved chemical speciation and source apportionment of organic aerosol components in Delhi, India, using extractive electro-spray ionization mass spectrometry, *Atmospheric Chemistry and Physics*, 22, 7739–7761, <https://doi.org/10.5194/acp-22-7739-2022>, 2022.
- 470 Lalchandani, V., Kumar, V., Tobler, A., M. Thamban, N., Mishra, S., Slowik, J. G., Bhattu, D., Rai, P., Satish, R., Ganguly, D., Tiwari, S., Rastogi, N., Tiwari, S., Močnik, G., Prévôt, A. S. H., and Tripathi, S. N.: Real-time characterization and source apportionment of fine particulate matter in the Delhi megacity area during late winter, *Science of The Total Environment*, 770, 145324, <https://doi.org/10.1016/j.scitotenv.2021.145324>, 2021.
- 475 Le Breton, M., Hallquist, Å. M., Pathak, R. K., Simpson, D., Wang, Y., Johansson, J., Zheng, J., Yang, Y., Shang, D., Wang, H., Liu, Q., Chan, C., Wang, T., Bannan, T. J., Priestley, M., Percival, C. J., Shallcross, D. E., Lu, K., Guo, S., Hu, M., and Hallquist, M.: Chlorine oxidation of VOCs at a semi-rural site in Beijing: significant chlorine liberation from ClNO₂ and subsequent gas- and particle-phase Cl–VOC production, *Atmospheric Chemistry and Physics*, 18, 13013–13030, <https://doi.org/10.5194/acp-18-13013-2018>, 2018.
- 480 Lee, B. H., Mohr, C., Lopez-Hilfiker, F. D., Lutz, A., Hallquist, M., Lee, L., Romer, P., Cohen, R. C., Iyer, S., Kurtén, T., Hu, W., Day, D. A., Campuzano-Jost, P., Jimenez, J. L., Xu, L., Ng, N. L., Guo, H., Weber, R. J., Wild, R. J., Brown, S. S., Koss, A., Gouw, J. de, Olson, K., Goldstein, A. H., Seco, R., Kim, S., McAvey, K., Shepson, P. B., Starn, T., Baumann, K., Edgerton, E. S., Liu, J., Shilling, J. E., Miller, D. O., Brune, W., Schobesberger, S., D’Ambro, E. L., and Thornton, J. A.: Highly functionalized organic nitrates in the southeast United States: Contribution to secondary organic aerosol and reactive nitrogen budgets, *PNAS*, 113, 1516–1521, <https://doi.org/10.1073/pnas.1508108113>, 2016.
- 485 Lopez-Hilfiker, F. D., Mohr, C., Ehn, M., Rubach, F., Kleist, E., Wildt, J., Mentel, T. F., Lutz, A., Hallquist, M., Worsnop, D., and Thornton, J. A.: A novel method for online analysis of gas and particle composition: description and evaluation of a Filter Inlet for Gases and AEROSols (FIGAERO), *Atmospheric Measurement Techniques*, 7, 983–1001, <https://doi.org/10.5194/amt-7-983-2014>, 2014.
- Meidan, D., Brown, S. S., Sinha, V., and Rudich, Y.: Nocturnal Atmospheric Oxidative Processes in the Indo-Gangetic Plain and Their Variation During the COVID-19 Lockdowns, *Geophysical Research Letters*, 49, e2021GL097472, <https://doi.org/10.1029/2021GL097472>, 2022.
- 490 Mishra, S., Tripathi, S. N., Kanawade, V. P., Haslett, S. L., Dada, L., Ciarelli, G., Kumar, V., Singh, A., Bhattu, D., Rastogi, N., Daellenbach, K. R., Ganguly, D., Gargava, P., Slowik, J. G., Kulmala, M., Mohr, C., El-Haddad, I., and Prevot, A. S. H.: Rapid night-time nanoparticle growth in Delhi driven by biomass-burning emissions, *Nat. Geosci.*, 16, 224–230, <https://doi.org/10.1038/s41561-023-01138-x>, 2023.
- 495 Morgan, W. T., Ouyang, B., Allan, J. D., Aruffo, E., Di Carlo, P., Kennedy, O. J., Lowe, D., Flynn, M. J., Rosenberg, P. D., Williams, P. I., Jones, R., McFiggans, G. B., and Coe, H.: Influence of aerosol chemical composition on N₂O₅ uptake: airborne regional measurements in northwestern Europe, *Atmospheric Chemistry and Physics*, 15, 973–990, <https://doi.org/10.5194/acp-15-973-2015>, 2015.
- Osthoff, H. D., Sommariva, R., Baynard, T., Pettersson, A., Williams, E. J., Lerner, B. M., Roberts, J. M., Stark, H., Goldan, P. D., Kuster, W. C., Bates, T. S., Coffman, D., Ravishankara, A. R., and Brown, S. S.: Observation of daytime N₂O₅ in the



- 500 marine boundary layer during New England Air Quality Study–Intercontinental Transport and Chemical Transformation 2004, *Journal of Geophysical Research: Atmospheres*, 111, <https://doi.org/10.1029/2006JD007593>, 2006.
- Osthoff, H. D., Roberts, J. M., Ravishankara, A. R., Williams, E. J., Lerner, B. M., Sommariva, R., Bates, T. S., Coffman, D., Quinn, P. K., Dibb, J. E., Stark, H., Burkholder, J. B., Talukdar, R. K., Meagher, J., Fehsenfeld, F. C., and Brown, S. S.: High levels of nitryl chloride in the polluted subtropical marine boundary layer, *Nature Geoscience*, 1, 324–328, <https://doi.org/10.1038/ngeo177>, 2008.
- 505 Pant, P., Shukla, A., Kohl, S. D., Chow, J. C., Watson, J. G., and Harrison, R. M.: Characterization of ambient PM_{2.5} at a pollution hotspot in New Delhi, India and inference of sources, *Atmospheric Environment*, 109, 178–189, <https://doi.org/10.1016/j.atmosenv.2015.02.074>, 2015.
- Priestley, M., Breton, M. le, Bannan, T. J., Worrall, S. D., Bacak, A., Smedley, A. R. D., Reyes-Villegas, E., Mehra, A., Allan, J., Webb, A. R., Shallcross, D. E., Coe, H., and Percival, C. J.: Observations of organic and inorganic chlorinated compounds and their contribution to chlorine radical concentrations in an urban environment in northern Europe during the wintertime, *Atmospheric Chemistry and Physics*, 18, 13481–13493, <https://doi.org/10.5194/acp-18-13481-2018>, 2018.
- 510 Rai, P., Furger, M., El Haddad, I., Kumar, V., Wang, L., Singh, A., Dixit, K., Bhattu, D., Petit, J.-E., Ganguly, D., Rastogi, N., Baltensperger, U., Tripathi, S. N., Slowik, J. G., and Prévôt, A. S. H.: Real-time measurement and source apportionment of elements in Delhi's atmosphere, *Science of The Total Environment*, 742, 140332, <https://doi.org/10.1016/j.scitotenv.2020.140332>, 2020.
- Riedel, T. P., Wolfe, G. M., Danas, K. T., Gilman, J. B., Kuster, W. C., Bon, D. M., Vlasenko, A., Li, S.-M., Williams, E. J., Lerner, B. M., Veres, P. R., Roberts, J. M., Holloway, J. S., Lefer, B., Brown, S. S., and Thornton, J. A.: An MCM modeling study of nitryl chloride (ClNO₂) impacts on oxidation, ozone production and nitrogen oxide partitioning in polluted continental outflow, *Atmospheric Chemistry and Physics*, 14, 3789–3800, <https://doi.org/10.5194/acp-14-3789-2014>, 2014.
- 520 Singh, A., Rastogi, N., Kumar, V., Slowik, J. G., Satish, R., Lalchandani, V., Thamban, N. M., Rai, P., Bhattu, D., Vats, P., Ganguly, D., Tripathi, S. N., and Prévôt, A. S. H.: Sources and characteristics of light-absorbing fine particulates over Delhi through the synergy of real-time optical and chemical measurements, *Atmospheric Environment*, 252, 118338, <https://doi.org/10.1016/j.atmosenv.2021.118338>, 2021a.
- Singh, N., Mhawish, A., Banerjee, T., Ghosh, S., Singh, R. S., and Mall, R. K.: Association of aerosols, trace gases and black carbon with mortality in an urban pollution hotspot over central Indo-Gangetic Plain, *Atmospheric Environment*, 246, 118088, <https://doi.org/10.1016/j.atmosenv.2020.118088>, 2021b.
- Slusher, D. L., Huey, L. G., Tanner, D. J., Flocke, F. M., and Roberts, J. M.: A thermal dissociation–chemical ionization mass spectrometry (TD-CIMS) technique for the simultaneous measurement of peroxyacyl nitrates and dinitrogen pentoxide, *Journal of Geophysical Research: Atmospheres*, 109, <https://doi.org/10.1029/2004JD004670>, 2004.
- 530 Spicer, C. W., Chapman, E. G., Finlayson-Pitts, B. J., Plastridge, R. A., Hubbe, J. M., Fast, J. D., and Berkowitz, C. M.: Unexpectedly high concentrations of molecular chlorine in coastal air, *Nature*, 394, 353–356, <https://doi.org/10.1038/28584>, 1998.
- Stewart, G. J., Nelson, B. S., Drysdale, W. S., Acton, W. J. F., Vaughan, A. R., Hopkins, J. R., Dunmore, R. E., Hewitt, C. N., Nemitz, E., Mullinger, N., Langford, B., Shivani, Reyes-Villegas, E., Gadi, R., Rickard, A. R., Lee, J. D., and Hamilton, J. F.: Sources of non-methane hydrocarbons in surface air in Delhi, India, *Faraday Discuss.*, 226, 409–431, <https://doi.org/10.1039/D0FD00087F>, 2021.
- 535



- Thornton, J. A., Mohr, C., Schobesberger, S., D'Ambro, E. L., Lee, B. H., and Lopez-Hilfiker, F. D.: Evaluating Organic Aerosol Sources and Evolution with a Combined Molecular Composition and Volatility Framework Using the Filter Inlet for Gases and Aerosols (FIGAERO), *Acc. Chem. Res.*, 53, 1415–1426, <https://doi.org/10.1021/acs.accounts.0c00259>, 2020.
- 540 Tobler, A., Bhattu, D., Canonaco, F., Lalchandani, V., Shukla, A., Thampan, N. M., Mishra, S., Srivastava, A. K., Bisht, D. S., Tiwari, S., Singh, S., Močnik, G., Baltensperger, U., Tripathi, S. N., Slowik, J. G., and Prévôt, A. S. H.: Chemical characterization of PM_{2.5} and source apportionment of organic aerosol in New Delhi, India, *Science of The Total Environment*, 745, 140924, <https://doi.org/10.1016/j.scitotenv.2020.140924>, 2020.
- 545 Wang, D. S. and Hildebrandt Ruiz, L.: Chlorine-initiated oxidation of *n*-alkanes under high-NO_x conditions: insights into secondary organic aerosol composition and volatility using a FIGAERO–CIMS, *Atmospheric Chemistry and Physics*, 18, 15535–15553, <https://doi.org/10.5194/acp-18-15535-2018>, 2018.
- Wang, H., Lu, K., Tan, Z., Sun, K., Li, X., Hu, M., Shao, M., Zeng, L., Zhu, T., and Zhang, Y.: Model simulation of NO₃, N₂O₅ and ClNO₂ at a rural site in Beijing during CAREBeijing-2006, *Atmospheric Research*, 196, 97–107, <https://doi.org/10.1016/j.atmosres.2017.06.013>, 2017.
- 550 Wang, L., Slowik, J. G., Tripathi, N., Bhattu, D., Rai, P., Kumar, V., Vats, P., Satish, R., Baltensperger, U., Ganguly, D., Rastogi, N., Sahu, L. K., Tripathi, S. N., and Prévôt, A. S. H.: Source characterization of volatile organic compounds measured by proton-transfer-reaction time-of-flight mass spectrometers in Delhi, India, *Atmospheric Chemistry and Physics*, 20, 9753–9770, <https://doi.org/10.5194/acp-20-9753-2020>, 2020.
- 555 Wolfe, G. M., Marvin, M. R., Roberts, S. J., Travis, K. R., and Liao, J.: The Framework for 0-D Atmospheric Modeling (F0AM) v3.1, *Geoscientific Model Development*, 9, 3309–3319, <https://doi.org/10.5194/gmd-9-3309-2016>, 2016.
- World Health Organization: WHO global air quality guidelines. Particulate matter (PM_{2.5} and PM₁₀), ozone, nitrogen dioxide, sulfur dioxide and carbon monoxide., 2021.
- 560 Yan, C., Tham, Y. J., Zha, Q., Wang, X., Xue, L., Dai, J., Wang, Z., and Wang, T.: Fast heterogeneous loss of N₂O₅ leads to significant nighttime NO_x removal and nitrate aerosol formation at a coastal background environment of southern China, *Science of The Total Environment*, 677, 637–647, <https://doi.org/10.1016/j.scitotenv.2019.04.389>, 2019.
- Ye, C., Yuan, B., Lin, Y., Wang, Z., Hu, W., Li, T., Chen, W., Wu, C., Wang, C., Huang, S., Qi, J., Wang, B., Wang, C., Song, W., Wang, X., Zheng, E., Krechmer, J. E., Ye, P., Zhang, Z., Wang, X., Worsnop, D. R., and Shao, M.: Chemical characterization of oxygenated organic compounds in the gas phase and particle phase using iodide CIMS with FIGAERO in urban air, *Atmospheric Chemistry and Physics*, 21, 8455–8478, <https://doi.org/10.5194/acp-21-8455-2021>, 2021.
- 565 Zhang, B., Shen, H., Yun, X., Zhong, Q., Henderson, B. H., Wang, X., Shi, L., Gunthe, S. S., Huey, L. G., Tao, S., Russell, A. G., and Liu, P.: Global Emissions of Hydrogen Chloride and Particulate Chloride from Continental Sources, *Environ. Sci. Technol.*, 56, 3894–3904, <https://doi.org/10.1021/acs.est.1c05634>, 2022.
- 570 Zhang, Y., Vu, T. V., Sun, J., He, J., Shen, X., Lin, W., Zhang, X., Zhong, J., Gao, W., Wang, Y., Fu, T. M., Ma, Y., Li, W., and Shi, Z.: Significant Changes in Chemistry of Fine Particles in Wintertime Beijing from 2007 to 2017: Impact of Clean Air Actions, *Environ. Sci. Technol.*, 54, 1344–1352, <https://doi.org/10.1021/acs.est.9b04678>, 2020.